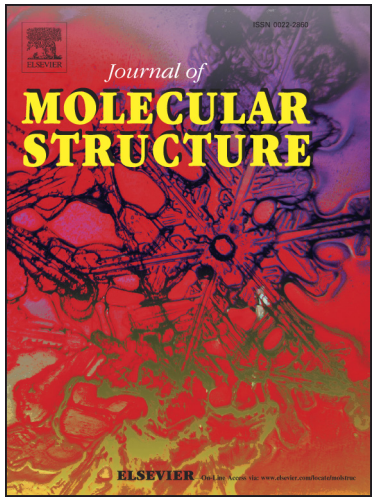

Biscoumarin derivatives: Synthesis, crystal structure, theoretical studies and induced apoptosis activity on bladder urothelial cancer cell

Jia-jia Xin, Jing Li, Zi-dan Zhang, Xing-bin Hu, Ming-kai Li

PII: S0022-2860(14)01227-7
DOI: http://dx.doi.org/10.1016/j.molstruc.2014.12.024
Reference: MOLSTR 21174

To appear in: *Journal of Molecular Structure*

Received Date: 31 August 2014
Revised Date: 5 December 2014
Accepted Date: 5 December 2014

Please cite this article as: J-j. Xin, J. Li, Z-d. Zhang, X-b. Hu, M-k. Li, Biscoumarin derivatives: Synthesis, crystal structure, theoretical studies and induced apoptosis activity on bladder urothelial cancer cell, *Journal of Molecular Structure* (2014), doi: http://dx.doi.org/10.1016/j.molstruc.2014.12.024

Biscoumarin derivatives: synthesis, crystal structure, theoretical studies and induced apoptosis activity on bladder urothelial cancer cell

Jia-jia Xin[1§], Jing Li[2§], Zi-dan Zhang[4], Xing-bin Hu[1*], Ming-kai Li[3*]

1. Department of Blood Transfusion, Xijing Hospital, the Fourth Military Medical University, Xi'an, China
2. School of Chemistry and Chemical Engineering, Xi'an University, Xi'an, China
3. Department of Pharmacology, School of Pharmacy, the Fourth Military Medical University, Xi'an, China
4. Department of Physics, School of Science, Tianjin University, Tianjin, China

[§]These authors contributed equally to this work.
[*]Corresponding author: mingkai@fmmu.edu.cn (Ming-kai Li) and hxbsxk@fmmu.edu.cn (Xing-bin Hu)

Abstract

In this study, five new biscoumarin derivatives (1~5) were synthesized and compound 4 inhibited the proliferation of the bladder urothelial cells (J82 cell line) obviously after 48 hours treatment at different concentration (1, 5 and 10 μmol/L), and J82 cells were predominantly induced to apoptotic cell death after compound 4 treatment. Morphologic changes of bladder urothelial cancer cells were also observed under transmission electron microscopy (TEM) after compound 4 treatment. In addition, compound 4 had much less toxicity to human umbilical vein endothelial cells. To explore the possible anti-cancer mechanism of compound 4, two classical intramolecular O—H···O hydrogen bonds (HBs) in their structures and the corresponding HB energies were performed with the density functional theory (DFT) [B3LYP/6-31G*] method. Anti-bladder cancer activity of compound 4 is possible due to the intramolecular weakest HB energies.

Key Words Biscoumarin, Crystal, Bladder urothelial cancer, Apoptosis, Chemotherapy

1. Introduction

Bladder urothelial cancer is diagnosed at an increasing rate in the world, which is the second most common urologic malignancy, while the clinical outcomes remain highly controversial [1-3]. Treatment for the bladder urothelial cancer takes different approaches depending on the conditions, and chemotherapy is one of the important treatments, which may be used before surgery, after surgery, or instead of surgery for those cases in which surgery is considered unsuitable [4-6]. However, chemotherapeutic agents against bladder urothelial cancer are still limited, more novel anti-cancer agents with great selectivity and specificity need to be developed for bladder urothelial cancer treatment.

Biscoumarins have received considerable attention in the past few years for their versatile biological and medical properties, such as antioxidant, anti-inflammatory, antibacterial, and anticancer activities [7-9]. It was reported that biscoumarin derivatives can strongly inhibit tubulin aggregation and played an efficient role against cancer, so the cancer cells were able to prevent progression through the cell cycle. Other mechanism of anti-cancer activity was due to the antiangiogenesis and promotion of apoptosis [10-12]. These results indicated that coumarin derivatives might represent interesting novel drug candidates.

In this work, we synthesized five new biscoumarin derivatives, namely,

3,3′-benzylidene-bis-(4-hydroxycoumarin) (1), 3,3′-(2-nitrobenzylidene)-bis-(4-hydroxycoumarin) (2), 3,3′-(3-nitrobenzylidene)-bis-(4-hydroxycoumarin) (3), 3,3′-(2-chloro-5-nitrobenzylidene)-bis-(4-hydroxycoumarin) (4) and 3,3′-(3-nitro-4-hydroxybenzylidene)-bis-(4-hydroxycoumarin) (5) (Fig. 1), and then evaluated their anti-cancer activities on two human bladder urothelial cell lines. In addition, the cell cycle analysis and apoptosis change induced by compound treatment were also observed.

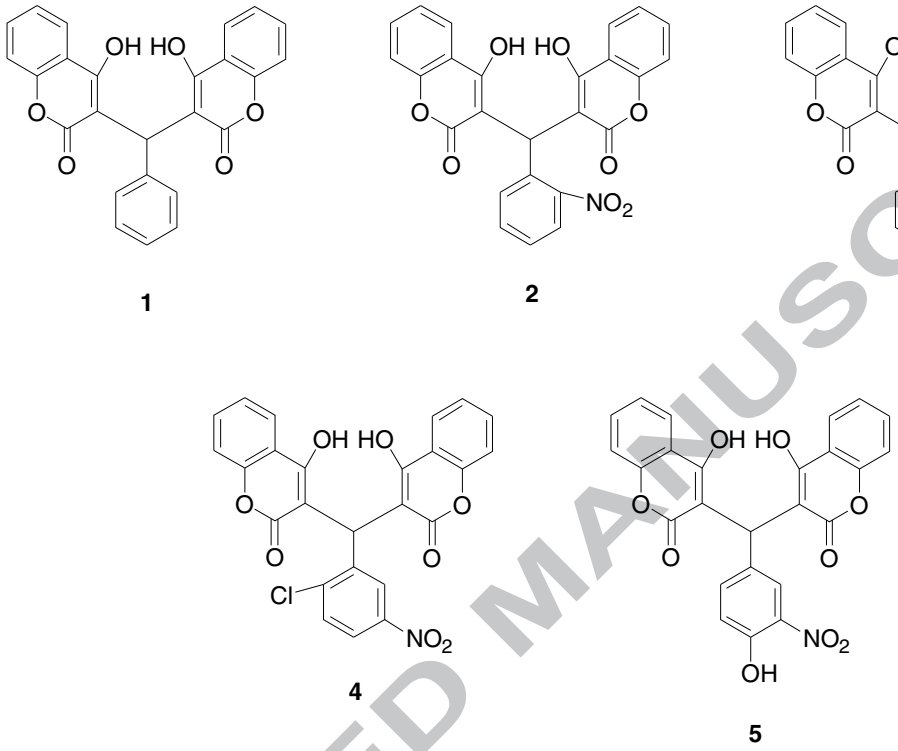

Fig. 1 Chemical structures of compounds 1~5

2. Experimental

2.1 Apparatus and materials

IR spectra (400-4000 cm^{-1}) were obtained using a Brucker Equinox-55 spectrophotometer. ^1H NMR spectra were obtained using a Varian Inova-400 spectrometer (at 400 MHz). Mass spectra were obtained using a micrOTOF-Q II mass spectrometer. The melting points were taken on a XT-4 micro melting apparatus, and the thermometer was uncorrected.

The bladder urothelial carcinoma cell line J82 and human umbilical vein endothelial cells were purchased from ATCC (Manassas, VA, USA). Cells were initially transferred into uncoated plastic tissue plates and were grown in Eagle's minimal essential medium (EMEM) with Earle's balanced salt solution (BSS) and 2 mM L-glutamine, modified to contain 1.0 mM sodium pyruvate, 0.1 mM nonessential amino acids, 1.5 g/L sodium bicarbonate, and 10% FBS. Cells were incubated at 37 °C in 95% air/5% CO_2. Medium was refreshed 3 times per week, and the cancer cells were harvested when they formed a confluent monolayer on the tissue plate.

2.2 Synthesis and characterization of compounds 1~5

Compounds 1~5 were synthesized according to a reported procedure [13]. A mixture of benzaldehyde (2-nitrobenzaldehyde, 3-nitrobenzaldehyde, 2-chloro-5-nitrobenzaldehyde and 3-nitro-4-hydroxybenzaldehyde) (10 mmol) and 4-hydroxycoumarin (20 mmol) was dissolved in 100 mL of EtOH. A few drops of piperidine were added, and the mixture was stirred for 3 h at room temperature. After reaction completion as determined by TLC,

water was added until precipitation occurred. After filtering the precipitates, they were sequentially washed with ice-cooled water and ethanol and then dried in a vacuum.

3,3′-Benzylidene-bis-(4-hydroxycoumarin) (1): m.p. 208-209 °C. IR (KBr pellet cm^{-1}): 3446 (OH), 1652 (C=O), 1615 (C-O), 1572 (C=C) cm^{-1}. ^1H NMR ($CDCl_3$, δ, ppm): 11.528 (s, 1H, OH), 11.299 (s, 1H, OH), 7.994-8.080 (q, 2H), 7.606-7.649 (m, 2H), 7.215-7.421 (m, 9H), 6.104 (s, 1H, CH). HRMS (ESI^+): *m/z*: calcd for $C_{25}H_{16}O_6$: 435.0839 [$M+Na^+$]; found: 435.0899.

3,3′-(2-Nitrobenzylidene)-bis-(4-hydroxycoumarin) (2): m.p. 218-219 °C. IR (KBr pellet cm^{-1}): 3446 (OH), 1652 (C=O), 1615 (C-O), 1520 (C=C) cm^{-1}. ^1H NMR ($CDCl_3$, δ, ppm): 11.550 (s, 1H, OH), 11.219 (s, 1H, OH), 7.978-8.073 (m, 2H), 7.612-7.658 (m, 3H), 7.540-7.582 (m, 1H), 7.386-7.464 (m, 6H), 6.628 (s, 1H, CH). HRMS (ESI^+): *m/z*: calcd for $C_{25}H_{15}NO_8$: 480.0690 [$M+Na^+$]; found: 480.0611.

3,3′-(3-Nitrobenzylidene)-bis-(4-hydroxycoumarin) (NBH): m.p. 220-221 °C. IR (KBr pellet cm^{-1}): 3446 (OH), 1652 (C=O), 1615 (C-O), 1555 (C=C) cm^{-1}. ^1H NMR ($CDCl_3$, δ, ppm): 11.579 (s, 1H, OH), 11.384 (s, 1H, OH), 8.137-8.162 (m, 1H), 8.070-8.104 (t, 2H), 7.990-8.008 (d, 1H), 7.651-7.690 (t, 2H), 7.568-7.591 (m, 1H), 7.496-7.536 (t, 1H), 7.385-7.453 (m, 4H), 6.129 (s, 1H, CH). HRMS (ESI^+): *m/z*: calcd for $C_{25}H_{15}NO_8$: 480.0690 [$M+Na^+$]; found: 480.0689.

3,3′-(2-Chloro-5-nitrobenzylidene)-bis-(4-hydroxycoumarin) (CBH): m.p. 150-151 °C. IR (KBr pellet cm^{-1}): 3489 (OH), 1684 (C=O), 1623 (C-O), 1520 (C=C) cm^{-1}. ^1H NMR ($CDCl_3$, δ, ppm): 11.752 (s, 1H, OH), 11.006 (s, 1H, OH), 8.359-8.365 (t, 1H), 8.064-8.144 (m, 3H), 7.640-7.683 (m, 2H), 7.533-7.555 (d, 1H), 7.402-7.438 (t, 4H), 6.192 (s, 1H, CH). HRMS (ESI^+): *m/z*: calcd for $C_{25}H_{14}ClNO_8$: 514.0300 [$M+Na^+$]; found: 514.0321.

3,3′-(3-Nitro-4-hydroxybenzylidene)-bis-(4-hydroxycoumarin) (NHH): m.p. 238-239 °C. IR (KBr pellet cm^{-1}): 3251 (OH), 1655 (C=O), 1582 (C-O), 1536 (C=C) cm^{-1}. ^1H NMR ($CDCl_3$, δ, ppm): 11.593 (s, 1H, OH), 11.396 (s, 1H, OH), 10.545-10.558 (d, 1H), 7.944-8.108 (m, 3H), 7.686 (s, 2H), 7.402-7.466 (m, 4H), 7.287 (s, 1H), 7.142-7.176 (q, 1H), 6.046 (s, 1H, CH). HRMS (ESI^+): *m/z*: calcd for $C_{25}H_{15}NO_9$: 496.0639 [$M+Na^+$]; found: 496.0632.

2.3 Crystal structure determination

For X-ray diffraction experiments, single crystals of compound 4 were both grown from methanol. The X-ray diffraction data were collected on a Bruker SMART APEX II CCD diffractometer equipped with a graphite monochromated Mo Kα radiation (λ = 0.71073 Å) by using the ω-2θ scan technique at room temperature. The structure was solved by direct methods using SHELXS-97 and refined using the full-matrix least squares method on F^2 with anisotropic thermal parameters for all non-hydrogen atoms by using SHELXL-97 [14]. Hydrogen atoms were generated geometrically. The crystal data and details concerning data collection and structure refinement are given in Table 1. Molecular illustrations were prepared using the XP package. Parameters in CIF format are available as Electronic Supplementary Publication from Cambridge Crystallographic Data Centre.

Table 1 Crystal data, data collection and structure refinement of compound 4

Formula	$C_{25}H_{14}ClNO_8$
*M*r	491.0408
Temperature / K	293(2)
Crystal system	Triclinic
Space group	$P\bar{1}$
a / Å	9.7912(9)
b / Å	11.2742(8)
c / Å	12.0934(13)
α / °	64.872(9)
β / °	79.063(9)
γ / °	84.199(7)

V / Å^3	1186.36(19)
Z	4
D_{calc} / g·cm^{-3}	1.506
μ(Mo Kα) / mm^{-1}	0.221
θ range / °	2.60 to 25.00
Reflections collected	7797
No. unique data[R(int)]	4179
No. data with $I \geq 2\sigma(I)$	3229[0.0210]
R_1	0.0657
ωR_2(all data)	0.2044
CCDC	1009072

2.4 Quantum chemical calculations

All calculations were carried out using the Gaussian 09 package [15]. Density functional theory (DFT), Becke's three-parameter hybrid function (B3LYP), and LYP correlation function were used to fully optimize all the geometries on the energy surface without constraints. Frequency calculations using the same basis sets have been performed to confirm that the stationary points are minima (zero imaginary frequencies) on the potenial energy surface. To obtain precise results that are in conjunction with experimental results, three basis sets, namely 6-31G*, 6-31+G**, and 6-311G*, were tested. Frequency calculations at the B3LYP (with basis sets 6-31G*) level of theory were carried out to confirm stationary points as minima and to obtain the zero-point energies and the thermal correlation data at 1 atm and 298 K.

2.5 Anti-cancer and cytotoxic activity assay

The anti-cancer activity of compounds to the bladder urothelial carcinoma cells (J82 cell line), and the in vitro cytotoxicity of compound to the human umbilical vein endothelial cells (HUVECs) was determined by 3-(4,5-dimethyl-2-thiazolyl)-2,5-diphenyl-2-H-tetrazolium bromide (MTT) staining as described previously [16]. Briefly, cells (5×10^3 cells/well) were seeded in a 96-well plate with 100 μL EMEM media with 20% fetal bovine serum (FBS) in every well for 12 hours, and then treated with or without compounds at various concentrations for 24 or 48 hours. After treatment, MTT solution (final concentration, 0.5%) was added and cells were incubated for another 4 hours at 37°C. 150 μL DMSO was added to each well after removal of the supernatant and the absorbance at 490 nm was measured with a microplate reader.

2.6 Detection of apoptosis by flow cytometry

The apoptotic ratios of cells were determined with the Annexin V-FITC apoptosis detection kit (Sigma, St. Louis, MO, USA) [17]. Briefly, after 48 hours compound 4 treatment, the cells were collected and washed twice with cold PBS buffer, resuspended in 100 mL of binding buffer, incubated with 5 mL of Annexin V conjugated to FITC and 10 mL PI for 15 min at room temperature, and analyzed by flow cytometry. Cells treated with DMSO were used as the negative control.

2.7 Transmission electron microscopy (TEM) observation

Bladder urothelial cancer cells were seeded and grown at 5×10^7/ml in three flasks. Cells after treated with compound 1 (1, 5 and 10 μmol/L) were harvested and washed with 1xPBS twice, and then added to 2.5% glutaraldehyde fixative for microtome sectioning using ultramicrotome (LKB-V; JEOL Co; Japan). TEM was performed with a Transmission Electron Microscope (JEM-2000EX; JEOL Co; Japan).

3 Results

3. 1 Molecular structure

The crystal structure of compound 4 is given in Fig. 2. The selected bond lengths, bond angles and partial values of torsional angles are listed in Table 2. From the diagram of the asymmetric unit including the atomic

numbering scheme of compound 4, we can see an ethanol solvent molecule incorporated in the asymmetric unit. The title compound is a 4-hydroxycoumarin dimer, consisting of two monomeric building blocks of 4-hydroxycoumarin and a 2-chloro-5-nitrophenyl ring on the central methylene linker. Two 4-hydroxycoumarin residues arranged in a position that permits the formation of two classical intramolecular hydrogen bonds between a hydroxyl group of one coumarin fragment and a lacton carbonyl group of another coumarin fragment help stabilize the whole structure [$d(O_3\text{-}O_4)$ = 2.575 Å and $d(O_1\text{-}O_6)$ = 3.429 Å].

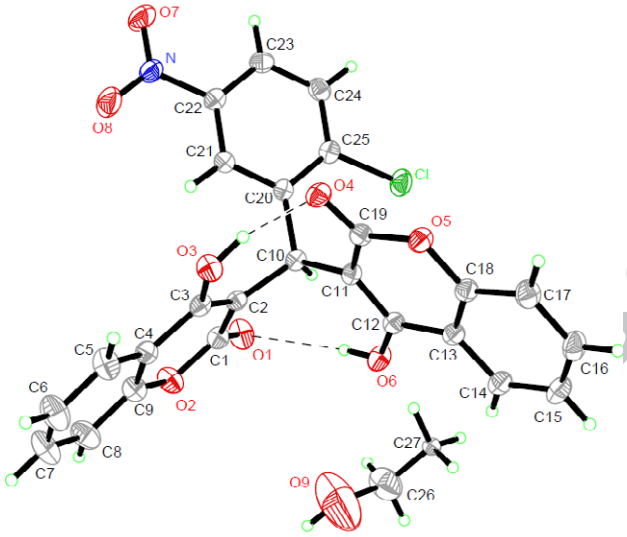

Fig. 2 Molecular structure of 3,3′-(2-chloro-5-nitrobenzylidene)-bis-(4-hydroxycoumarin) (4).

3.2 Quantum chemical calculations

3.2.1 Geometric parameters of compounds 1~5

The fully optimized molecular structures of compounds 1~5 with atomic numbering calculated at B3LYP level of theory are shown in Fig. 3. For compound 4, selected calculated geometric parameters under three different basis sets (6-31G*, 6-31+G**, and 6-311G*) and experimental geometric parameters are presented in Table 2.

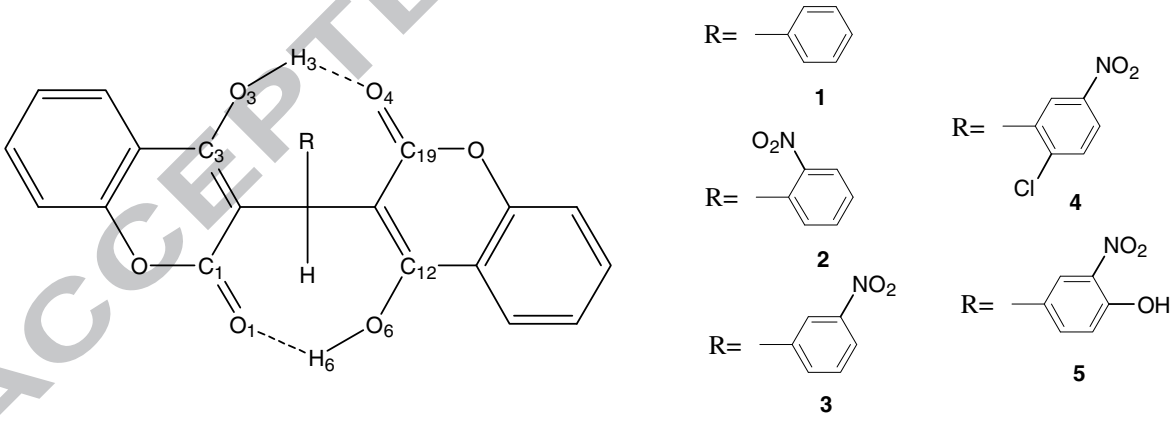

Fig. 3 Schematic presentation of compounds 1~5

As seen in Table 2, the calculated geometric parameters of compound 4 agree with available experimental data. Under three different basis sets, the maximum deviation of the selected bond lengths and bond angles are very close; the average discrepancy of the selected bond lengths between theoretical and experimental data is less than ±0.02Å, and the average discrepancy of the selected bond angles is less than ±2°. B3LYP/6-31G* exhibited sufficient agreement with experimental data and lower computational cost, so further theoretical study was performed at this level.

Table 2 Experimental and calculated parameters of the selected bond lengths and bond angles of 3,3′-(2-chloro-5-nitrobenzylidene)-bis-(4-hydroxycoumarin) (4).

Name definition	X-ray	6-31G*	6-31+G**	6-311G*
$R(C_{19}=O_4)$	1.221	1.232	1.235	1.224
$R(C_1=O_1)$	1.205	1.233	1.236	1.226
$R(C_1\text{-}O_2)$	1.370	1.370	1.367	1.369
$R(C_9\text{-}O_2)$	1.374	1.368	1.370	1.367
$R(C_{19}\text{-}O_5)$	1.358	1.372	1.370	1.372
$R(C_{18}\text{-}O_5)$	1.370	1.367	1.369	1.365
$R(C_{10}\text{-}C_{20})$	1.525	1.539	1.540	1.538
$A(C_1\text{-}C_2\text{-}C_{10})$	115.33	114.05	114.05	113.80
$A(C_3\text{-}C_2\text{-}C_{10})$	125.55	126.24	126.41	126.43
$A(C_{10}\text{-}C_{11}\text{-}C_{19})$	120.46	119.91	119.77	119.35
$A(C_{10}\text{-}C_{11}\text{-}C_{12})$	119.94	120.73	121.01	121.19
$A(C_2\text{-}C_{10}\text{-}C_{11})$	113.33	112.18	111.97	112.02
$A(C_2\text{-}C_{10}\text{-}C_{20})$	115.24	114.66	115.18	115.02
$A(C_{11}\text{-}C_{10}\text{-}C_{20})$	113.45	116.95	116.38	116.41
$D(C_3\text{-}C_2\text{-}C_{10}\text{-}C_{11})$	56.57	62.11	62.34	61.22
$D(C_2\text{-}C_{10}\text{-}C_{11}\text{-}C_{19})$	98.57	102.87	102.33	103.45
$D(C_1\text{-}C_2\text{-}C_{10}\text{-}C_{20})$	104.79	102.23	102.67	101.33
$D(C_{19}\text{-}C_{11}\text{-}C_{10}\text{-}C_{20})$	40.32	45.22	45.33	46.12

3.2.2 Estimation of the single and total HB energies in compounds 1~5

To obtain single and total HB energies of the five compounds, structure optimization was performed to elucidate stable PES structures.

We took compound 4 for example to estimate single and total HB energies. The global minimum structure is stabilized by two HBs (4ab); however, two higher energy structures is stabilized by one HB (4a or 4b) respectively.

The relative energies of different structures were calculated to estimate the strengths of the HBs formed. The O_6—H_6···O_1 HB energy was estimated from the energy difference between 4ab and 4a, $E(O_6—H_6\ldots O_1)=E_{4ab}^{coor}-E_{4a}^{coor}$, calculated to be -42.905921 kJ/mol (Table 3). 4a is a global minimum structure with one HB (O_3—H_3···O_4). The O_3—H_3···O_4 HB energy was estimated from the energy difference between 4ab and 4b, $E(O_3—H_3\ldots O_4)=E_{4ab}^{coor}-E_{4b}^{coor}$, calculated to be -50.231066 kJ/mol (Table 3). 4b was obtained from the global minimum structure, but H_3 was rotated around the C_3—O_3 bond until O_3—H_3···O_4 HB rupture occurred [18, 19]. The HB energies obtained predicted that O_3—H_3···O_4 HB is stronger than O_6—H_6···O_1, which is consistent with the fact that the distance of O_3—O_4 is greatly shorter than that of O_6—O_1. The total HB energy in compound 4 was estimated to be -93.136987 kJ/mol by the equation $2E_{4ab}^{coor}-(E_{4a}^{coor}+E_{4b}^{coor})$ (Table 3).

For compounds 1~3 and compound 5, their total HB energies are -118.4546835, -118.215763, -115.5666335 and -120.3450435 kJ·mol^{-1}, respectively (Table 3).

Table 3 Total electronic energies (in hartree) and HB energies (in kJ/mol) of hydrogen bonded conformers of compounds 1~5 calculated at B3LYP/6-31G* level of theory.

System	Total electronic energies[a]	$E(O_6—H_6\cdots O_1)$	$E(O_3—H_3\cdots O_4)$	E(total HB)
1ab	-1413.328042			-118.4546835
1a	-1413.308121	-52.3025855		
1b	-1413.302846		-66.152098	
2ab	-1617.817382			-118.215763
2a	-1617.799287	-47.5084225		
2b	-1617.790451		-70.7073405	
3ab	-1617.827653			-115.5666335
3a	-1617.807773	-52.19494		
3b	-1617.803516		-63.3716935	
4ab	-2077.424463			-93.136987
4a	-2077.408121	-42.905921		
4b	-2077.405331		-50.231066	
5ab	-1567.108786			-120.3450435
5a	-1567.088785	-52.5126255		
5b	-1567.08295		-67.832418	

[a] ZP corrected.

3.3 Effect of compounds on the viability of bladder urothelial cancer cells

After treatment with compounds 1~5 (0.1, 1, 5 and 10 μmol/L) for 48 h, cell viability was decreased in bladder urothelial cell line J82 at 1, 5 and 10 μmol/L significantly(Table 4), and compound 4 showed the most potent anti-cancer activities on the J82 cells. A probity analysis of the dose–response functions showed the IC_{50} value of compound 4 was 7.36±2.47μmol/L.

Table 4 Effect of compounds 1~5 on the J82 cell viability

Compounds	Value relative to control (%)			
(μmol/L)	0.1	1	5	10

1	99.36±8.57	91.21±8.84	88.36±6.95	79.38±8.42
2	97.94±5.83	86.38±7.56	80.86±6.51	72.68±7.85
3	97.42±6.65	88.51±6.74	79.57±5.88	70.13±4.69
4	90.36±8.05	80.12±7.74*	36.46±5.33*	33.31±6.06**
5	98.56±6.16	92.58±5.56	83.16±5.42	71.38±7.26

3.4 Induction of apoptosis by compound 4 in J82 cell line

To determine whether the treatment of cells using compound 4 may lead to apoptotic cell death, Annexin V-FITC/PI staining flow cytometric analysis was performed. After compound 4 treatment for 48 hours, cell apoptosis was observed in J82 cell line. Apoptosis was seen in only 2.34± 0.38% of vehicle treated control cells (Fig. 4), after treatment with 1 μmol/L compound 4, the apoptotic cells ration was 11.17± 0.44%, and when the cells were treated with 5 and 10 μmol/L compound 4, it was increased dramatically to 63.17±6.38 and 66.35±8.17, respectively.

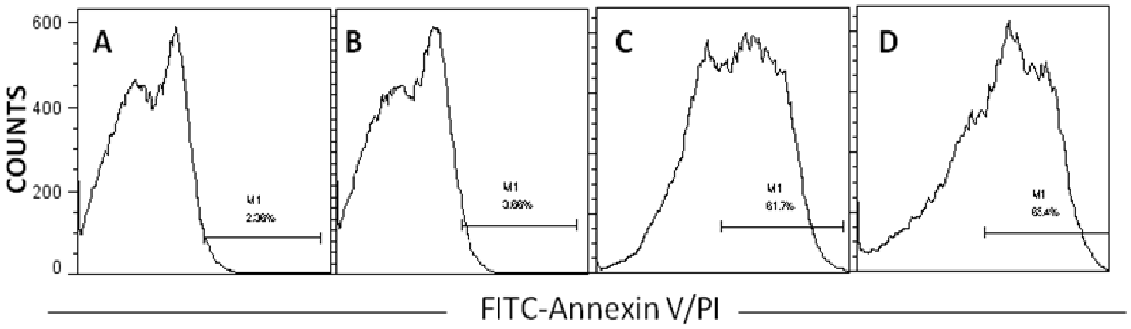

Fig. 4 Compound 4 induce apoptosis in J82 cell line. A: Control J82 cells without treatment of compound 4; B: Cells were treated with 1 μmol/L compound 4 for 48 hours; C: Cells were treated with 5 μmol/L compound 4 for 48 hours; D: Cells were treated with 10 μmol/L compound 4 for 48 hours. Induction of apoptosis was determined using Annexin V FITC/propidium iodide staining. Data was from at least three independent experiments.

3.5 Induction of apoptosis by compound 4 in J82 cell

Under the observation of transmission electron microscope, bladder urothelial cancer J82 cells were round and regular, with abundant organelles and normal double-membrane nuclei (Fig. 5A). After exposing to compound 4 for 24 hours, early stage apoptosis could be observed in 1 μmol/L (Fig. 5B) compound 4 treatment, and more apoptosis change could be observed in 5 μmol/L (Fig. 5C) and 10 μmol/L (Fig. 5D) compound 4 treatment group. It showed that nuclear membrane was domed outward with a sharp angle, and the nuclei chromatin was concentrated and clustered on the inner border of cells. The endoplasmic reticulum became dilated in the inner segment.

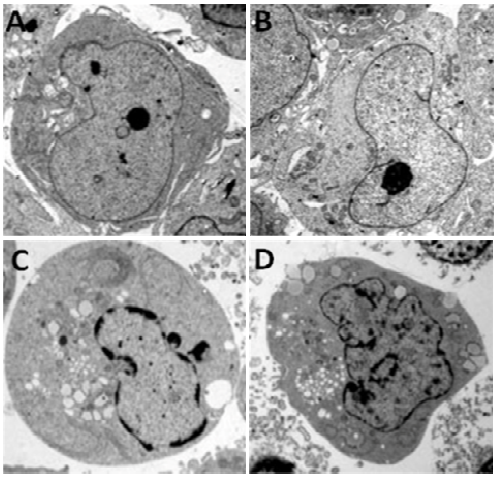

Fig. 5 Transmission electron microscopy showed J82 cell morphologic change of compound 4 treatment. A: Control; B: Treated with 1μmol/L compound 4; C: Treated with 5μmol/L compound 4; D: Treated with 10 μmol/L compound 4.

3.6 Cytotoxic activity of compound 4 on HUVECs

To further explore the safety of compound 4, we investigated its cytotoxicity to the HUVECs in vitro. As shown in Fig. 6, after treated with the compound 4 for 24 hours or 48 hours, there was no significant difference on cell viability between the control group and compound 4 treated group under concentration of 100 μmol/L ($P > 0.05$). These results implied that compound 4 had much less toxicity to mammalian normal endothelial cells, and had a relatively wide safety range for potential anticancer applications.

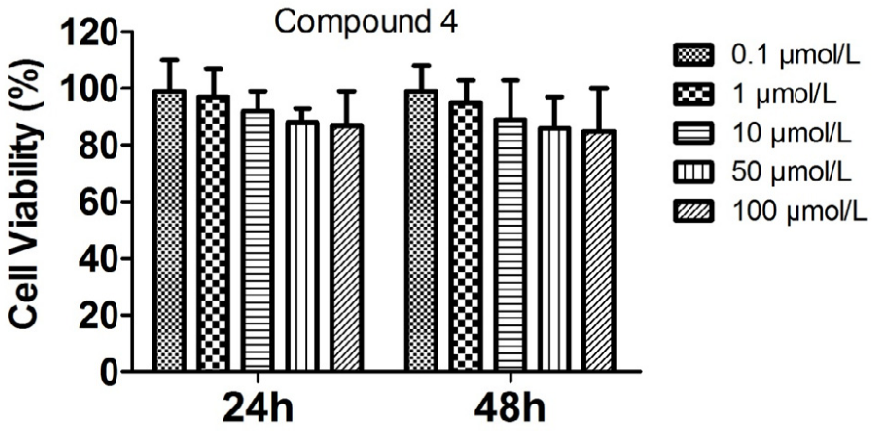

Fig. 6 Effect of compound 4 on the viability of HUVECs cells as determined by MTT assay. Data are represented as mean percentage of viable cells in bars ± SD of at least three replicates in six independent tests.

4. Discussion

Bladder urothelial cancer patients are suffering from limited treatment options due to late diagnosis and poor drug tolerance [20, 21]. Therefore, it is significant for us to seek novel chemotherapy agent which can effectively prevent the disease and even eradicate the progression and metastasis of bladder urothelial cancer.

In this study, we have demonstrated that new biscoumarin derivatives suppressed cell proliferation in J82 bladder urothelial cancer cells. In addition, it was discovered firstly that the compound 4 had bladder urothelial cancer cell cytotoxicity by promoting the apoptosis death. In agreement with our results, it was reported that

coumarin derivative could induce the apoptosis and inhibit proliferation in the other cancers such as lung cancer and colon cancer [22, 23].

X-ray structural analysis also showed that all the compounds were stabilized by two asymmetrical intramolecular O—H···O HBs, which were considered as important factors in assisting the molecule to attain the correct configuration for biological activity [22, 23]. Our study also firstly demonstrated that the energy of hydrogen bonds in compounds 1~5 were in agreement with their anti-proliferation activity in vitro. The total HB stabilization energies in compounds 1~5 were estimated to be -118.4546835, -118.215763, -115.5666335, -93.136987, -120.3450435 kJ/mol, respectively. These values suggest that the most potent anti-cancer activity in compound 4 was consistent with its weakest HB strengths.

5. Conclusion

Taken together, our study demonstrated the in vitro therapeutic effect of biscoumarin derivatives on human bladder urothelial cancer J82 cell line, suggesting that biscoumarin derivative is a potential therapeutic drug for bladder urothelial cancer. Furthermore, biscoumarin derivatives can inhibit bladder urothelial cancer cells growth through anti-proliferation and induce apoptosis. In compounds 1~5, compound 4 had the most potent anti-cancer efficiency, possibly because two strong electron-withdrawing groups (NO_2 and Cl) on the phenyl ring further weakens the HB strengths. However, it will be beneficial and necessary for further study to reveal the underlying mechanism and study the effect in vivo.

Acknowledgments

This work was supported by grants from the project of science and technology of Shaanxi Province (2012K13-02-26). The authors thank the High Performance Computing Center of Tianjin University and Prof. Xuehao He for the services provided.

Reference

[1] T.O. Al Hussain, M. Akhtar, Adv. Anat. Pathol. 20 (2013) 53.
[2] V. Radosavljevic, G. Belojevic, Tumori. 100 (2014) 1.
[3] A. Onishi, D. Sugiyama, S. Kumagai, A. Morinobu, Arthritis Rheum. 65 (2013) 1913.
[4] E.M. Carballido, J.E. Rosenberg, Curr. Oncol. Rep. 16 (2014) 404.
[5] H.Z. Kaimakliotis, M.F. Monn, K.C. Cary, J.A. Pedrosa, K. Rice, T.A. Masterson, T.A. Gardner, N.M. Hahn, R.S. Foster, R. Bihrle, L. Cheng, M.O. Koch, Urol. Oncol. 32 (2014) 833.
[6] D.L. Willis, T.W. Flaig, D.E. Hansel, M.I. Milowsky, R.L. Grubb, H.A. Al-Ahmadie, E.R. Plimack, T.M. Koppie, D.J. McConkey, C.P. Dinney, V.A. Hoffman, M.J. Droller, E. Messing, A.M. Kamat, Urol. Oncol. 32 (2014) 826.
[7] N. Au, A.E. Rettie, Drug Metab. Rev. 40 (2008) 355.
[8] M.K. Li, J. Li, B.H. Liu, Y. Zhou, X. Li, X.Y. Xue, Z. Hou, X.X. Luo, Eur. J. Pharmacol. 721 (2013) 151.
[9] F. Pérez-Cruz, S. Serra, G. Delogu, M. Lapier, J.D. Maya, C. Olea-Azar, L. Santana, E. Uriarte, Bioorg. Med. Chem. Lett. 22 (2012) 5569.
[10] N.H. Kim, S.N. Kim, J.S. Oh, S. Lee, Y.K. Kim, Biochem. Biophys. Res. Commun. 418 (2012) 616.
[11] S.N. Kim, N.H. Kim, Y.S. Park, H. Kim, S. Lee, Q. Wang, Y.K. Kim, Biochem. Pharmacol. 77 (2009) 1773.
[12] H. Madari, D. Panda, L. Wilson, R.S. Jacobs, Cancer Res. 63 (2003) 1214.
[13] N. Hamdi, M.C. Puerta, P. Valerga. Eur. J. Med. Chem. 43 (2008) 2541.
[14] G.M. Sheldrick, SHELXL-97, Program for Solution Crystal Structure and Refinement, University of Göttingen, Germany, 1997.
[15] Gaussian 09, Revision A.02, M.J. Frisch, G.W. Trucks, H.B. Schlegel, G.E. Scuseria, M.A. Robb, J.R. Cheeseman, G. Scalmani, V. Barone, B. Mennucci, G.A. Petersson, H. Nakatsuji, M. Caricato, X. Li, H.P.

Hratchian, A.F. Izmaylov, J. Bloino, G. Zheng, J.L. Sonnenberg, M. Hada, M. Ehara, K. Toyota, R. Fukuda, J. Hasegawa, M. Ishida, T. Nakajima, Y. Honda, O. Kitao, H. Nakai, T. Vreven, J.A. Montgomery, Jr., J.E. Peralta, F. Ogliaro, M. Bearpark, J.J. Heyd, E. Brothers, K.N. Kudin, V.N. Staroverov, R. Kobayashi, J. Normand, K. Raghavachari, A. Rendell, J.C. Burant, S.S. Iyengar, J. Tomasi, M. Cossi, N. Rega, J.M. Millam, M. Klene, J.E. Knox, J.B. Cross, V. Bakken, C. Adamo, J. Jaramillo, R. Gomperts, R.E. Stratmann, O. Yazyev, A.J. Austin, R. Cammi, C. Pomelli, J.W. Ochterski, R.L. Martin, K. Morokuma, V.G. Zakrzewski, G.A. Voth, P. Salvador, J.J. Dannenberg, S. Dapprich, A.D. Daniels, O. Farkas, J.B. Foresman, J.V. Ortiz, J. Cioslowski, and D.J. Fox, Gaussian, Inc., Wallingford CT, 2009.

[16] C. Vasconcelos-Nóbrega, R. Pinto-Leite, R. Arantes-Rodrigues, R. Ferreira, P. Brochado, M.L. Cardoso, C. Palmeira, A. Salvador, C.I. Guedes-Teixeira, A. Colaço, L.F. Palomino, C. Lopes, L. Santos, P.A. Oliveira, Urol. Oncol. 31 (2013) 1212.

[17] A.P. Demchenko, Exp. Oncol. 34 (2012) 263.

[18] F. Koga, M. Yokoyama, H. Fukushima, Expert. Rev. Anticancer Ther. 13 (2013) 1269.

[19] G. Giannarini, F.D. Birkhäuser, F. Recker, G.N. Thalmann, U.E. Studer, Eur. Urol. 65 (2014) 825.

[20] Vijay Avin BR, Thirusangu P, Lakshmi Ranganatha V, Firdouse A, Prabhakar BT, Khanum SA, Eur J Med Chem.75 (2014)211.

[21] Zhang W, Li Z, Zhou M, Wu F, Hou X, Luo H, Liu H, Han X, Yan G, Ding Z, Li R,Bioorg Med Chem Lett.24(2014)799..

[22] J.C. Jung, S. Oh, Molecules 17 (2011) 240.

[23] J.C. Jung, E. Lim, Y. Lee, D. Min, J. Ricci, O.S. Park, M. Jung, Molecules 17 (2012) 2091.

Highlights

1．Five new biscoumarin derivatives (1~5) were synthesized.

2．Their anti-cancer activities on two human bladder urothelial cell lines were evaluated.

3．The cell cycle analysis and apoptosis change of the compounds were also observed.

4．The HB energies of compounds 1~5 were calculated.